

# Role of late winter mesoscale events in the biogeochemical variability of the upper water column of the North Pacific Subtropical Gyre

R. M. Letelier,<sup>1</sup> D. M. Karl,<sup>2</sup> M. R. Abbott,<sup>1</sup> P. Flament,<sup>2</sup> M. Freilich,<sup>1</sup>  
R. Lukas,<sup>2</sup> and T. Strub<sup>1</sup>

**Abstract.** Continuous records of upper water column (0–150 m) temperature profiles, spectral distribution of downwelling irradiance, and phytoplankton solar-induced fluorescence at 25 m depth were obtained during the inaugural deployment of the Hawaii Air-sea Logging Experiment, A Long-term Oligotrophic Habitat Assessment (HALE ALOHA) mooring, near the Hawaii Ocean Time-series (HOT) Station ALOHA (22°45'N; 158°00'W). The temperature record showed a strong upwelling event in March–April 1997, displacing the thermocline by 120 m. Remote sensing satellite (NSCAT and TOPEX/ERS 2) analyses suggest that the observed upwelling was a result of strong wind divergence and the passage of a cyclonic eddy through the HOT program study area. At the onset of the upwelling event increases in colored dissolved organic matter (CDOM) and chlorophyll fluorescence efficiency in the upper water column were detected by changes in the spectral distribution of the downwelling irradiance. The 0–25 m mean chlorophyll *a* (chl *a*) concentration increased threefold toward the end of the upwelling period. Water column samples collected during the monthly HOT cruises also indicate that the relative contribution of diatoms to total chl *a* increased twofold inside the eddy. The long-term temporal variability in frequency and intensity of these poorly resolved mesoscale events might be key factors determining the structure of the pelagic ecosystem in the North Pacific Subtropical Gyre. Integrating multi-year remote sensing satellite, moored, and vessel-based time series records permits a quantification of the spatial and temporal scale of upper water column perturbations and the characterization of the pelagic ecosystem response at various timescales.

## 1. Introduction

Biological processes control many geochemical patterns in the ocean. For this reason, and for predictive modeling purposes, a complete understanding of ecological responses to environmental perturbations in marine pelagic environments is imperative. This has been crucial for the study of mechanisms responsible for controlling biogeochemical cycles [DeAngelis, 1992]. However, the relevant time scales and space scales of response to variability are different for physiological, population and community parameters. Furthermore, the questions, methods, results and conclusions derived from any given study are predetermined by the scale of interest [Dayton and Tegner, 1984]. In other words, knowledge derived from large-scale studies does not necessarily provide an understanding of small-scale variability, or vice versa. Nevertheless, both the short-term response of populations to transient shifts in the physicochemical environment and the long-term evolution of the community in response to climate change are important aspects of the role of marine pelagic ecosystems in biogeochemical cycles.

Organic matter produced via photosynthesis is the primary energy available to organisms. Hence, both short- and long-term variations in the rate of photosynthesis will affect the biological activity of the community. In large regions of the ocean, net primary production (i.e., the amount of energy derived from photosynthesis that is available to higher trophic levels [Falkowski *et al.*, 1998]) is controlled by the rate of supply of physical and biogeochemical variability not routinely resolved by the monthly cruise sampling design. This experiment was dubbed Hawaii Air-sea Logging Experiment at Station ALOHA, or simply HALE ALOHA (the Hawaiian meaning of hale is “at the house of”). Among other equipment, HALE ALOHA-I was outfitted with meteorological instruments on the surface buoy, an optical sensor, a gas tension device, and 10 thermistors distributed in the upper 150 m of the water column (Table 1). During March and April 1997 these instruments recorded significant temporal changes in the upper water column light field, associated with a strong upward doming of the isothermal field. Changes in the temperature and density fields, as well as in the chl *a* and nutrient depth distribution were also observed during regular HOT cruises that were periodically conducted throughout this 4-month observation period. Remote sensing satellite data analyses suggest that the changes observed in the water column resulted from the combined effects of wind stress and the passage of a cyclonic eddy or frontal meander. In the present paper we have used these different time series data sets to describe and interpret the different temporal scale of response of phytoplankton assemblages to mesoscale perturbations in the North Pacific Subtropical Gyre.

<sup>1</sup> College of Oceanic and Atmospheric Sciences, Oregon State University, Corvallis

<sup>2</sup> School of Ocean and Earth Science and Technology, University of Hawaii, Honolulu

**Table 1.** HALE ALOHA-I Instrument Configuration

| Depth, m | Quantity | Description                                   | Model   | Manufacturer   | Scientists                   |
|----------|----------|---|---------|----------------|------------------------------|
| Surface  | 2        | Marine anemometer                             | 5106    | R.M. Young     | P. Flament and<br>M. Sawyer  |
|          | 2        | Meteorological probe with multi-plate shield  | MP101A  | Rotronic       |                              |
|          | 1        | Rain gauge                                    | 50203   | R.M. Young     |                              |
|          | 1        | Precision spectral pyranometer                | PSP     | Eppley Labs    |                              |
|          | 1        | Air/water temperature difference thermocouple | N/A     | N/A            |                              |
| 2        | 2        | Data logger with high stability thermistor    | XX-105  | RBR            | D. Karl and<br>T. Houlihan   |
| 38       | 1        | Data logger with high stability thermistor    | XX-105  | RBR            |                              |
| 50       | 1        | Data logger with high stability thermistor    | XX-105  | RBR            |                              |
| 60       | 1        | Data logger with high stability thermistor    | XX-105  | RBR            |                              |
| 80       | 1        | Data logger with high stability thermistor    | XX-105  | RBR            |                              |
| 100      | 1        | Data logger with high stability thermistor    | XX-105  | RBR            |                              |
| 120      | 1        | Data logger with high stability thermistor    | XX-105  | RBR            |                              |
| 130      | 1        | Data logger with high stability thermistor    | XX-105  | RBR            |                              |
| 150      | 1        | Data logger with high stability thermistor    | XX-105  | RBR            |                              |
| 25       | 1        | Downwelling irradiance spectroradiometer      | OCI-200 | Satlantic      | M. Abbott and<br>R. Letelier |
| 50       | 1        | Gas tension / Seacat                          | N/A     | N/A            | S. Emerson and<br>C. Stump   |
| 120      | 1        | Nitrate osmoanalyzer                          | N/A     | N/A            | H. Jannasch                  |
| 180      | 1        | Nitrate osmoanalyzer                          | N/A     | N/A            |                              |
| 410      | 1        | Seacat  | SBE-16  | SeaBird Elect. | R. Lukas and<br>C. Nosse     |
| 475      | 1        | Seacat  | SBE-16  |                |                              |
| 540      | 1        | Seacat  | SBE-16  |                |                              |
| 560      | 1        | Seacat  | SBE-16  |                |                              |
| 650      | 1        | Seacat  | SBE-16  |                |                              |
| 785      | 1        | Seacat  | SBE-16  |                |                              |

## 2. Methods

### 2.1. Moored Data Acquisition

One downwelling irradiance spectroradiometer (Satlantic, Inc., Halifax, Nova Scotia, Canada) equipped with an Alpha-Omega datalogger (Alpha-Omega, Corvallis, Oregon) and 10 Richard Brannker Research (RBR) XX-105 thermistors were deployed as components of the HALE ALOHA physical-biogeochemical mooring near Station ALOHA. HALE ALOHA is configured as a semi taut mooring with a surface 2.5 m diameter Guardian style buoy anchored in a 4800 m depth water column (Table 1). The approximate position of the mooring during its first deployment was 22°27'N and 158°08'W (Figure 1).

The spectroradiometer, placed at 25 m depth, measured downwelling irradiance every 20 min at seven discrete channels with 10 nm bandwidth centered at 412, 443, 490, 510, 555, 670 and 683 nm. To avoid changes in the downwelling light spectrum resulting from high solar angle, only measurements collected between 10:00 and 14:00 local time were used to estimate the mean 0-25 m chl *a* concentrations. Relative changes in colored dissolved organic matter (CDOM), as a proxy for newly upwelled seawater, and chlorophyll fluorescence efficiency (CFE), as a proxy for phytoplankton fluorescence quantum efficiency, were also calculated. Chl *a* concentrations were derived from the ratio between downwelling irradiance at 443 and 555 nm [Clark, 1981; Smith *et al.*, 1991] and calibrated relative to the 0-25 m mean chl *a* concentration measured by the fluorometric technique [Strickland and Parsons, 1972] using the HOT program core

measurement data. The resulting calibration based on a model II linear regression [Laws, 1997] gave

$$\text{chl } a \text{ (mg m}^{-3}\text{)} = 1.93 \text{ (Ed}_{443}\text{/Ed}_{555})^{-2.6}$$

$$r = 0.96, n = 8$$

nutrients into the euphotic zone [Denman, 1973; Lewis *et al.*, 1983; Platt *et al.*, 1992].

Variability in the rate of nutrient supply also has important effects on the fate of net primary production. Sudden inputs of nutrients into the euphotic zone can alter the balance between net and gross production and enhance rates of organic matter export due to the shift in the size of primary producers and the uncoupling between primary productivity and grazing [Landry *et al.*, 1997; Dugdale and Wilkerson, 1998]. Because the generation time of phytoplankton varies from hours to days [Steele, 1978; Harris, 1986; Falkowski *et al.*, 1998], these events produce short-lived (day-weeks) community perturbations that may be relevant in the sequestration of carbon dioxide from the atmosphere. These short-lived or "pulsed" perturbations may also play an important role in maintaining the observed complexity in the pelagic ecosystem structure [Odum *et al.*, 1995; Weigert and Penas-Lado, 1995]. However, if the same amount of nutrients is to be introduced at rates that do not allow uncoupling between primary productivity and grazing, a large fraction of these nutrients may become part of the recycling pool. Hence, the perturbation may produce long-term shifts in the community structure and the cycle of nutrients [Letelier *et al.*, 1996; Karl *et al.*, 1997; Karl, 1999].

The Hawaii Ocean Time-series (HOT) program was

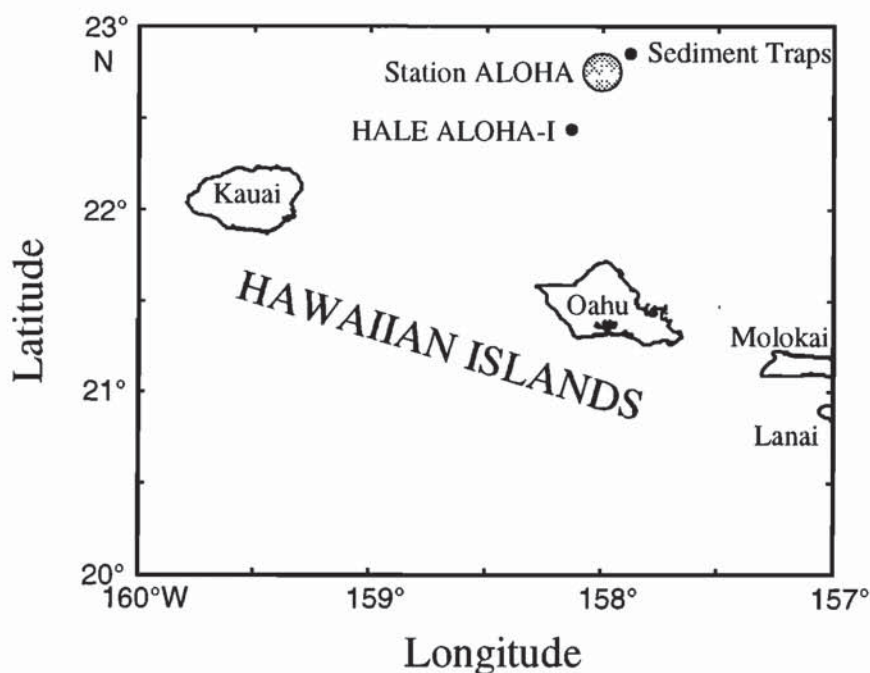


**Figure 1.** Map showing the positions of Station ALOHA (shaded circle with 11.1 km radius around 22°45'N, 158°W), HALE ALOHA-I (22°27'N, 158°08'W), and the ALOHA sediment trap mooring site (22°51'N, 157°53.7'W).

established in 1988 to monitor a set of key parameters that would characterize the physical processes controlling biogeochemical cycles in the oligotrophic North Pacific Subtropical Gyre [Karl and Lukas, 1996]. During the past decade the HOT program has helped to identify and quantify major mechanisms responsible for seasonal and interannual variability in chemistry and biology at Station ALOHA (22°45'N, 158°W; Figure 1) [Karl *et al.*, 1995, 1997; Dore and Karl, 1996; Letelier *et al.*, 1993, 1996]. However, the study of the plankton community response to sub-seasonal variability and its relevance in biogeochemical cycles in the upper water column has remained elusive, given that the main sampling frequency of the HOT program is approximately 10 five-day cruises per year.

Sediment-trap derived flux estimates, water column nutrient analyses, and inverted echo sounder records have independently documented sporadic mesoscale perturbations at Station ALOHA [Karl *et al.*, 1996; Chiswell, 1996]. These are important, but presently unresolved components of ecological variability [e.g., Dickey, 1991; Wiggert *et al.*, 1994; Lawson *et al.*, 1996]. The suggested ecological role for mesoscale processes is not new. Mesoscale processes may help to explain discrepancies between new production [e.g., Dugdale and Goering, 1967] and estimated fluxes of nitrate into the euphotic zone of oligotrophic oceans based on climatological mean conditions [Angel and Fasham, 1983; Platt and Harrison, 1985; Franks *et al.*, 1986; Hayward, 1987, 1991; Woods, 1988; Falkowski *et al.*, 1991; McGillicuddy and Robinson, 1997; McGillicuddy *et al.*, 1998; Oschlies and Garçon, 1998]. However, detailed field studies aimed at quantifying the ecosystem response to mesoscale perturbations and its effect on nutrient and carbon fluxes are rare due to the costs and logistics involved in sampling high-frequency, stochastic events.

In January 1997 a physical-biogeochemical mooring was deployed near Station ALOHA to observe that portion of the

where  $Ed_{443}$  and  $Ed_{555}$  are the measured downwelling irradiances at 443 and 555 nm, respectively.

In order to estimate relative changes in CDOM, Carder *et al.* [1991] and Siegel *et al.* [1995] used variations of the reflectance ratio between 410 and 441 nm and changes in the attenuation coefficient ratio between 410 and 488 nm, respectively. The underlying assumption of these two methods is that changes in these ratios are the result of a relative change in CDOM, which has an absorption spectrum in the visible region that increases exponentially with decreasing wavelength. In the present study we have taken a similar approach and used  $Ed_{443}/Ed_{412}$  and  $Ed_{490}/Ed_{412}$  to estimate relative changes in CDOM. These ratios strongly covary at Station ALOHA, indicating that the temporal trends observed are mainly the result of relative changes in the absorbance at 412 nm. CDOM concentrations cannot be estimated because not all dissolved organic matter has similar optical properties. The bleaching of CDOM under high light conditions [Nelson *et al.*, 1998] decreases the total amount of CDOM without necessarily altering dissolved organic matter (DOM) concentrations.

Chlorophyll fluorescence efficiency (CFE) was estimated based on Letelier *et al.* [1997] according to the following equation:

$$CFE = (Ed_{683} - Ed_{670}) / (Ed_{490} \text{ chl } a)$$

where  $Ed_{490}$ ,  $Ed_{670}$ , and  $Ed_{683}$  are the measured downwelling irradiances at 490, 670, and 683 nm, respectively.

This calculation assumes that all 683 nm energy measured at 25 m depth is derived from chlorophyll fluorescence. Irradiance at 670 nm is subtracted from the irradiance measured at 683 nm to account for any changes in background water values. However, this subtraction does not significantly change the temporal patterns of CFE.

In the present study, CFE is being used as a proxy for phytoplankton fluorescence quantum yield. Biophysical studies of terrestrial plants have determined that the fluorescence quantum yield ( $\Phi_f$ ) of the photochemical apparatus is inversely correlated to the photosynthesis quantum efficiency ( $\Phi_p$ ; Walker and Osmond, 1986). This inverse relationship has also been documented in the marine environment [Topliss and Platt, 1986] and can be explained by a competition of both pathways (fluorescence and carbon fixation) for electrons extracted from water during the light reaction [Krause and Weis, 1991; Kiefer and Reynolds, 1992]. Letelier et al. [1997] observed strong variations in CFE in the surface waters of an Antarctic cyclonic eddy and postulated that these variations were the result of changes in nutrient availability due to upwelling within the eddy. The field observations presented here confirm the utility of CFE analyses in detecting changes in the physiological status of phytoplankton assemblages.

A second assumption in the interpretation of CFE variations is that the phytoplankton assemblage is uniformly distributed in the upper 25 m of the water column. This uniformity is required because red light is strongly attenuated by water. While the spectroradiometer integrates the 0–25 m attenuation for the wavelengths used in the estimation of chl *a* concentration, it only detects chl *a* fluorescence in close proximity (< 2 m) [Kirk, 1994]. The large data set collected by the HOT program over the past decade ([http://hahana.soest.hawaii.edu/hot/hot\\_jgofs.html](http://hahana.soest.hawaii.edu/hot/hot_jgofs.html)) fully supports the assumption of a homogeneous chl *a* distribution over this depth interval.

Temporal changes in the depth resolved temperature fields were monitored by 10 thermistors deployed at 2, 38, 50, 60, 80, 100, 120, 130, and 150 m (duplicate sensors were deployed at 2 m depth). The sampling frequency was set at 30 min. A 31-hour filter was applied to the data in order to facilitate the comparison between mooring and shipboard observations (see below).

## 2.2. Research Vessel Data Collection and Analysis

The ship data discussed in this paper are a subset of the approximately monthly HOT program core measurements performed at Station ALOHA. A detailed description of these data sets is given by Karl and Lukas [1996]. During each cruise, high-resolution profiles of temperature, conductivity, fluorescence and dissolved oxygen are obtained using a Sea-Bird 911-plus conductivity-temperature-depth probe (CTD) equipped with several external and internal sensors. The CTD instrument package is mounted in an aluminum frame containing 24 polyvinyl chloride sample bottles.

In order to remove tidal and near-inertial period oscillations from single profiles, an average 0–1000 m density profile is derived from a repeated series of 12 to 18 hydrocasts collected at approximately 3-hour intervals, covering three semidiurnal tidal and a complete inertial period ( $f^{-1} = 31.03$  hours at Station ALOHA). In our present analysis the depth distributions of chl *a* and inorganic nutrients derived from single-cast profiles have been fitted to the cruise average density versus depth profile.

Chl *a* concentrations were determined by the fluorometric technique [Strickland and Parsons, 1972] as described by Letelier et al. [1996]. High performance liquid chromatography (HPLC) was used for the identification and quantification of accessory algal pigments, according to Latasa et al. [1997]. Dissolved inorganic nutrients including  $[\text{NO}_3^- + \text{NO}_2^-]$ , soluble reactive phosphorus [SRP] and soluble reactive silicate [SRSi] concentrations were determined on a four-channel autoanalyzer

[Karl and Lukas, 1996] except in near-surface waters (0–100 m) where high-sensitivity methods were required. In these lower nutrient regions, concentrations of  $[\text{NO}_3^- + \text{NO}_2^-]$  and SRP were measured by the chemiluminescent method [Garside, 1982] (as described by Dore and Karl [1996]) and the magnesium-induced coprecipitation method [Karl and Tien, 1992], respectively.

## 2.3. Remote Sensing Satellite Data Analysis

Data from two satellite altimeters are available for 1997: TOPEX/POSEIDON and ERS 2. The long-term mean height at each location was subtracted to remove the unknown marine geoid. Standard corrections were also applied to remove the effects of tides, orbital errors, and environmental factors (i.e., path delays caused by the ionosphere and atmosphere and changes in apparent sea level caused by waves), before combining the residual heights of both satellites to form mesoscale sea surface height fields. Furthermore, in order to compensate for differences in orbital errors between both satellites, the data had to be adjusted before being combined using the residual height field from two alternative sources: the U.S. National Aeronautic and Space Administration/National Oceanic and Atmospheric Administration (NASA/NOAA) Pathfinder project and the European office for archiving, validation, and interpretation of satellites oceanographic data (AVISO). Because the methods of removing the long-term mean, calculating orbital and tidal corrections are not identical, the fields produced from these two independent sources differ in fine detail but agree for scales larger than 100 km. Gridded residual height was formed using 35 days of data (one complete ERS 2 repeat and several TOPEX repeat cycles), centered every 5 days, as given by Strub and James [2000].

A review of scatterometry and descriptions of the NASA scatterometer (NSCAT) flight instrument and ground processing algorithms is given by Naderi et al. [1991]. The present study used 25 km resolution NSCAT wind measurements retrieved using the NSCAT 1 model function [Wentz and Smith, 1999] and a circular median filter ambiguity removal algorithm [Naderi et al., 1991, and references therein] with limited initialization from the operational National Centers for Environmental Prediction global surface wind analyses [Freilich, 1994]. Preliminary comparisons between NSCAT and HALE ALOHA buoy wind measurements indicate consistent quantitative accuracy in the HALE ALOHA location.

Spatially and temporally varying winds cause Ekman pumping in the oceanic and atmospheric boundary layers. The Ekman pumping associated with winds that vary only negligibly over an inertial period ( $f^{-1} = 31.43$  hours at the buoy location) was derived according to Gill [1982]. The time-dependent Ekman pumping equation is easily solved analytically in frequency space and, like the wind stress curl, the stress divergence forcing  $D_{\text{tau}}$  was calculated directly from the NSCAT measurements.

## 3. Results

The optical sensor package on the HALE ALOHA-I mooring recorded a significant increase in the concentration of chl *a* in the upper 25 m of the water column between March 21 and April 10, 1997 (Figure 2). Based on the empirical relationship derived from discrete chl *a* concentrations measured during the periodic HOT cruises and the corresponding 443 nm/555 nm irradiance ratios recorded by the moored spectroradiometer, the mean chl *a*

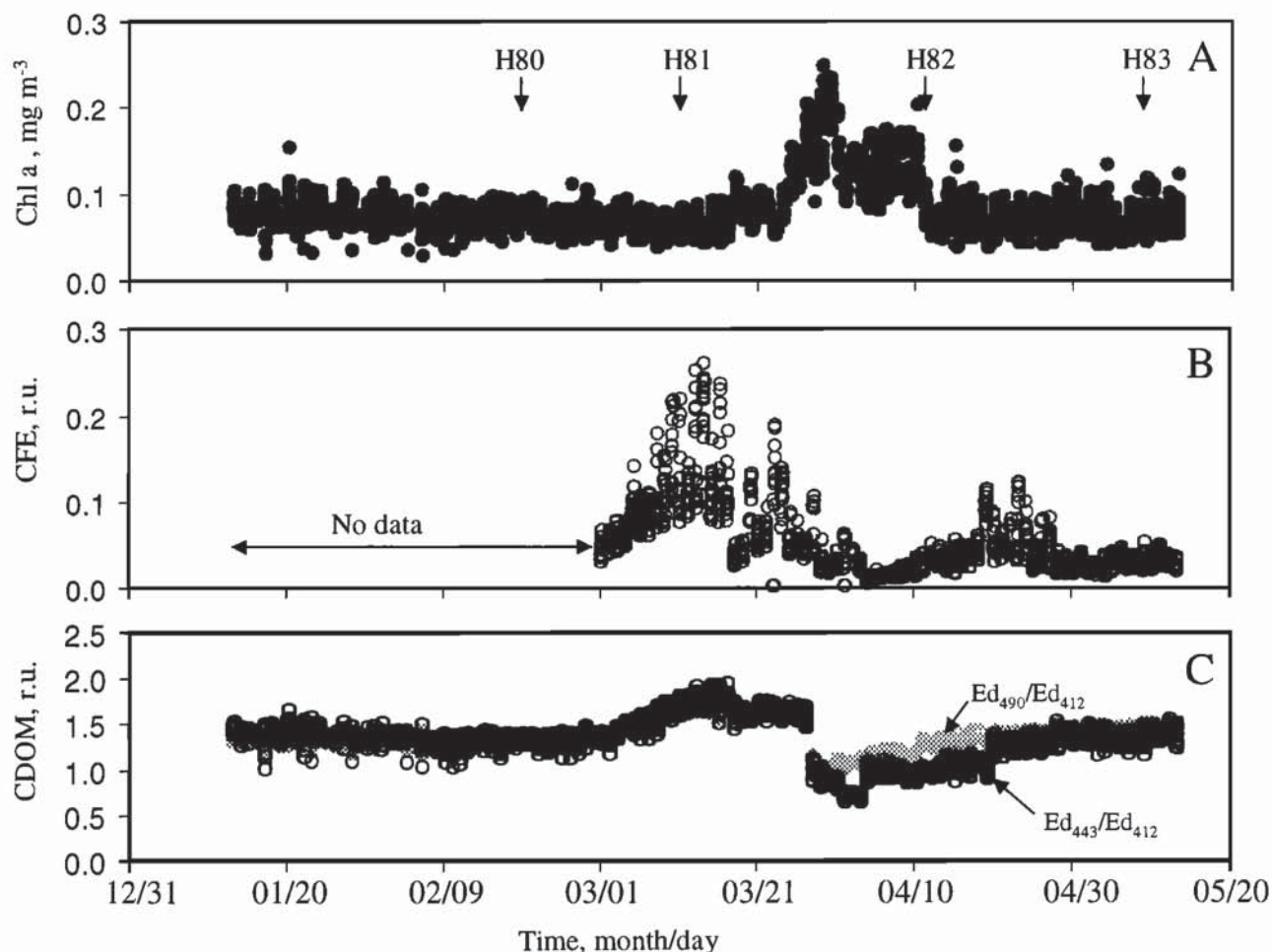


**Figure 2.** Temporal variations in (a) chlorophyll *a* concentration, (b) chlorophyll fluorescence efficiency (CFE), and (c) colored dissolved organic matter (CDOM) in the upper 25 m of the water column derived from moored spectrophotometric time series measurements and observations.

concentration in the upper 25 m reached  $0.26 \text{ mg chl } a \text{ m}^{-3}$  on March 30. This value corresponds to a threefold increase when compared to the mean  $0.07 \text{ mg chl } a \text{ m}^{-3}$  recorded between January 16 and March 20 by the moored spectroradiometer and the mean  $0.08 \text{ mg chl } a \text{ m}^{-3}$  obtained through fluorometric analyses over the first 9-year HOT field program (standard deviation =  $0.027 \text{ mg chl } a \text{ m}^{-3}$ ,  $n = 78$ ). The significant difference between the climatological mean condition and the perturbed condition suggests that these mesoscale, stochastic features are not well represented in the HOT program database.

The rise in chl *a* concentration was preceded by increases in CDOM and CFE, first observed on March 2 (Figure 2). While the maximum in CFE was recorded during the middle of March a secondary maximum was also observed during late April. The derived CDOM signal also displayed a maximum concentration during mid March, and then dropped abruptly by the end of the month.

The thermistor chain recorded a strong shoaling of the thermocline between March 2 and 28, followed by a deepening trend (Plate 1). This behavior of the thermocline during March and April is consistent with the passage of a cyclonic eddy or frontal meander during this period. The two TOPEX/ERS 2 satellite-derived altimeter fields (based on AVISO and Pathfinder

orbit error compensations) confirm the passage of a cyclonic feature (depressed surface height) during March and April 1997 (Plate 1b), centered around March 20–25, with a central height difference of approximately 20 cm compared to the reference height outside the feature of about 140 cm. The gridded topographic fields derived from both sources show a cyclonic eddy with a diameter of approximately 100–150 km, which passed from east to west with its center to the north of the mooring (Figures 3 and 4). In February, prior to the arrival of the eddy, an anticyclonic feature also passed from east to west, north of the mooring. The depression of isotherms associated with the passage of the anticyclonic feature was recorded by the mooring during February (Plate 1a), followed by the rise in isotherms during the passage of the cyclonic eddy in March–April. Both the anticyclonic and cyclonic signature of these eddies, clearly seen in the altimetry data, appear to be associated with the meandering of a zonal front north of the Hawaiian Islands (Figure 5). This subtropical zonal front is usually found further north in the Pacific but can be displaced southward during wintertime (Jeffrey Polovina, personal communication, 1999). This seasonal displacement may significantly increase the frequency of mesoscale perturbations affecting the surface waters of Station ALOHA by enhancing the vertical displacement of the water

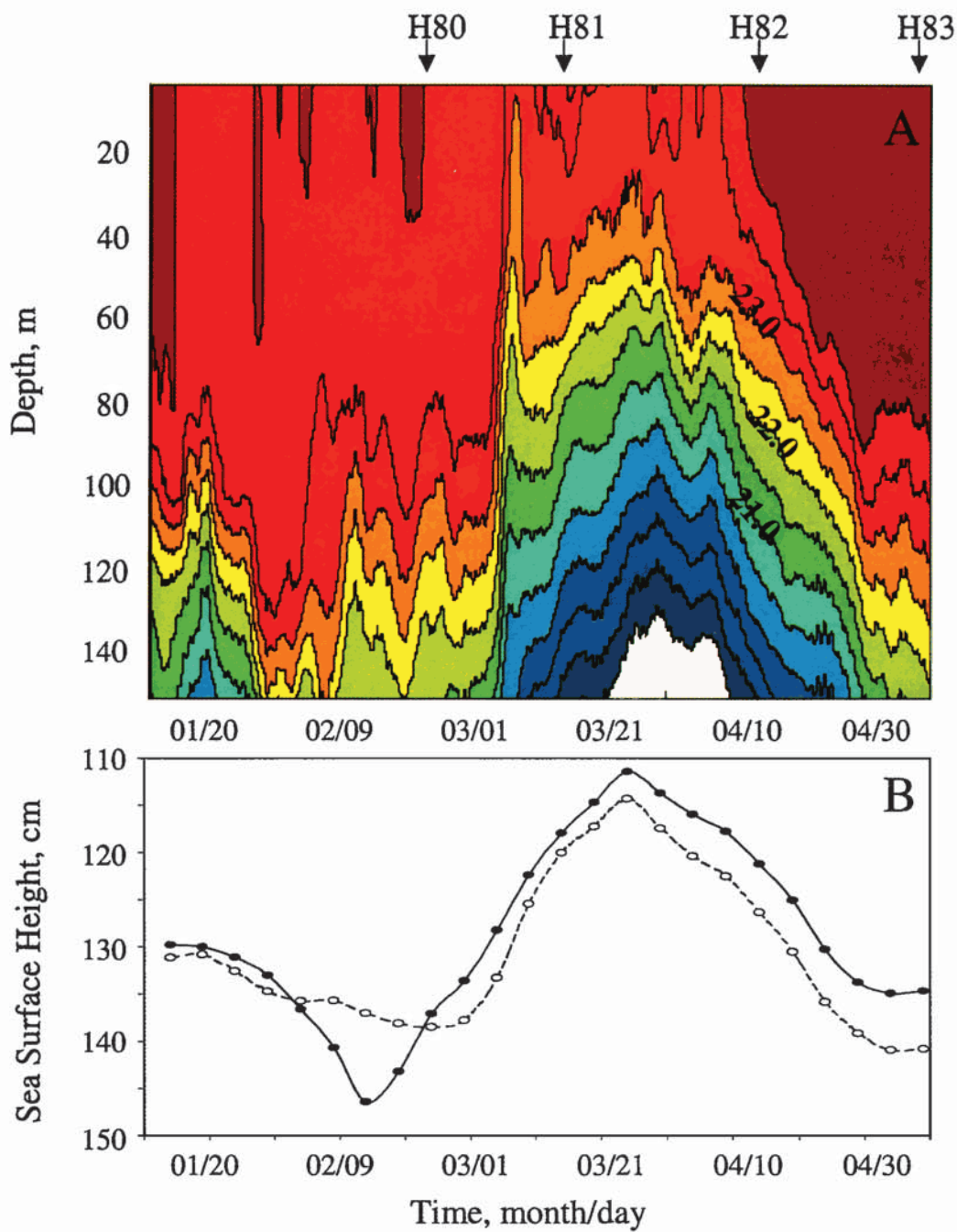


**Plate 1.** Time series displaying (a) 0–150 m depth distribution of temperature recorded by moored thermistors deployed at 2, 38, 50, 60, 80, 100, 120, 130 and 150 m and (b) sea surface height derived from TOPEX/ERS 2 and AVISO (solid) and TOPEX/ERS 2 and Pathfinder (dashed).

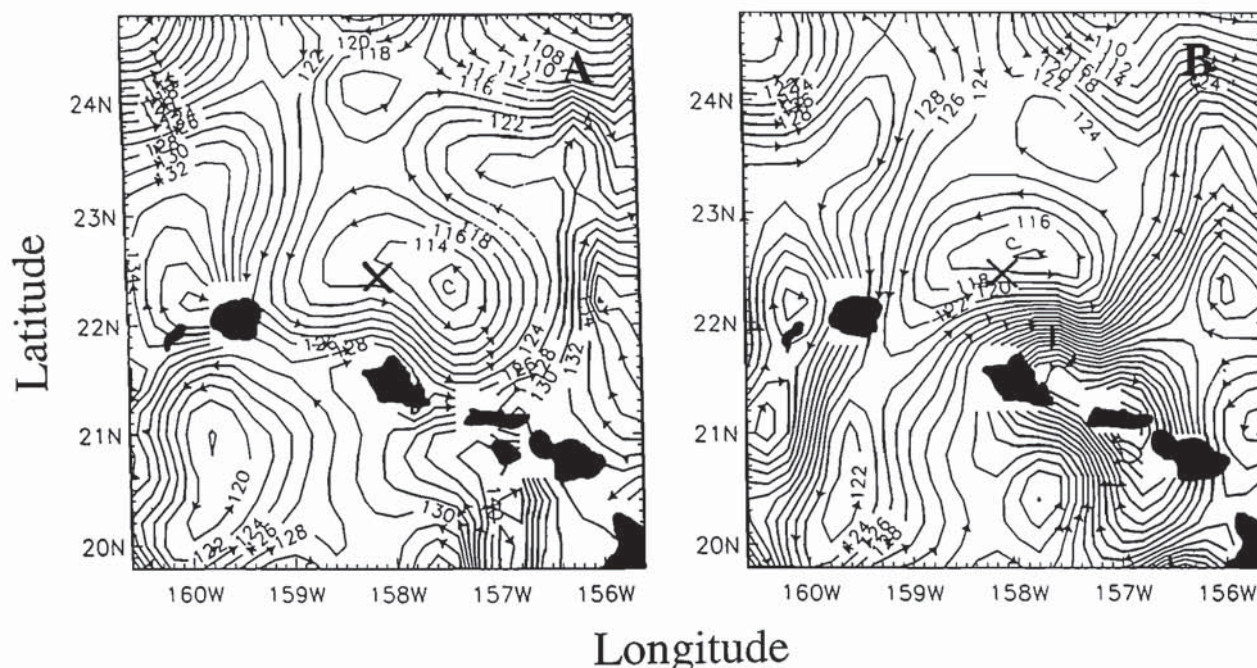


**Figure 3.** Maps of sea surface anomaly calculated for March 20, 1997, using (a) TOPEX/ERS 2 and AVISO and (b) TOPEX/ERS 2 and Pathfinder (the mooring position is marked with an X).

column as a result of an increased number of eddies passing by the station and by the upwelling and downwelling regimes associated with the meandering of the front.

The dramatic rise in isotherms (approximately 60 m during the 2-day period, March 5–6; Plate 1a) may have been the result of the combined effect of the cyclonic eddy and a strong wind-driven Ekman pumping event. The wind stress curl and derived Ekman pumping velocities from NSCAT wind scatterometry analyses indicate that a sea surface divergence resulting from wind forcing may have been a significant component (30%) of the burst event observed during March 5–6 (Figure 6). The coincidence therefore of a mesoscale eddy and a meteorological event may have altered significantly the upper water column habitat and this, in turn, affected the standing stock and productivity of the microbial assemblage.

Based on the thermistor records and the TOPEX/ERS 2 results, we can establish that, while the cruises HOT-81 (March 10–14) and HOT-82 (April 7–11) sampled a cyclonic eddy, HOT-80 (February 16–20) and HOT-83 (May 5–9) sampled the water column before and after the passage of this event, respectively. Depth profiles of  $\sigma_t$  collected during these periods display a shallowing of the pycnocline of approximately 100 m between February 18 and March 12 (HOT-80 and HOT-81, respectively; Figure 7). While depth distributions of  $\sigma_t$  are very similar for both cruises in which the eddy is sampled, suggesting only minor vertical displacements of the water column between HOT-81 and HOT-82,  $\sigma_t$  profiles collected during HOT-80 and HOT-83 are also similar. These observations hint at a symmetry in the temporal evolution of the position of the pycnocline between February 18 and May 7 (HOT-80 and HOT-83, respectively). However, this symmetry is lost when the chl *a* and nutrient depth distributions are analyzed (Figure 8). The only chl *a* profile significantly different during these four cruises is the one recorded during HOT-82 in which the deep chlorophyll maximum

layer (DCML) appears to be 40 m shallower than the 10 year HOT program climatological mean position (Figure 8a). Depth profiles of  $[\text{NO}_3^- + \text{NO}_2^-]$  (Figure 8b), SRP (Figure 8c), and SRSi (Figure 8d) display a continuous shoaling between HOT-80 and HOT-82 (65 m between HOT-80 and HOT-81 and 47 m between HOT-81 and HOT-82), followed by a 100 m deepening between HOT-82 and HOT-83.

#### 4. Discussion

Optimally, knowledge at physiological, population and community levels is required to evaluate the minimal temporal length of a perturbation perceived by a biological unit [Harris, 1986; Abbott and Letelier, 1998]. However, traditional shipboard studies are inadequate to sample properly all of the relevant scales of variability that collectively impact phytoplankton productivity and community structure. It is because of this inadequacy that short-term stochastic events in the North Pacific Subtropical Gyre have been undersampled historically and that the conceptual view of a stable climax community [e.g., Krebs, 1985] has been used in describing the North Pacific Subtropical Gyre pelagic ecosystem.

The advent of satellite oceanography and the development of moored sensors led to the discovery of ubiquitous mesoscale features in the world's oceans. However, despite their usefulness in detecting and mapping mesoscale and larger scales of variability, remote sensing data are still difficult to interpret from a biogeochemical perspective unless concurrent in situ observations and chemical and microbial water analyses are also performed. The data set described herein is one of the most observation-intensive mesoscale events ever studied in the North Pacific Subtropical Gyre. Furthermore, these integrated observations have continued to the present with some enhanced measurement capabilities. The only time series measurement no longer available is the wind scatterometry, which terminated with

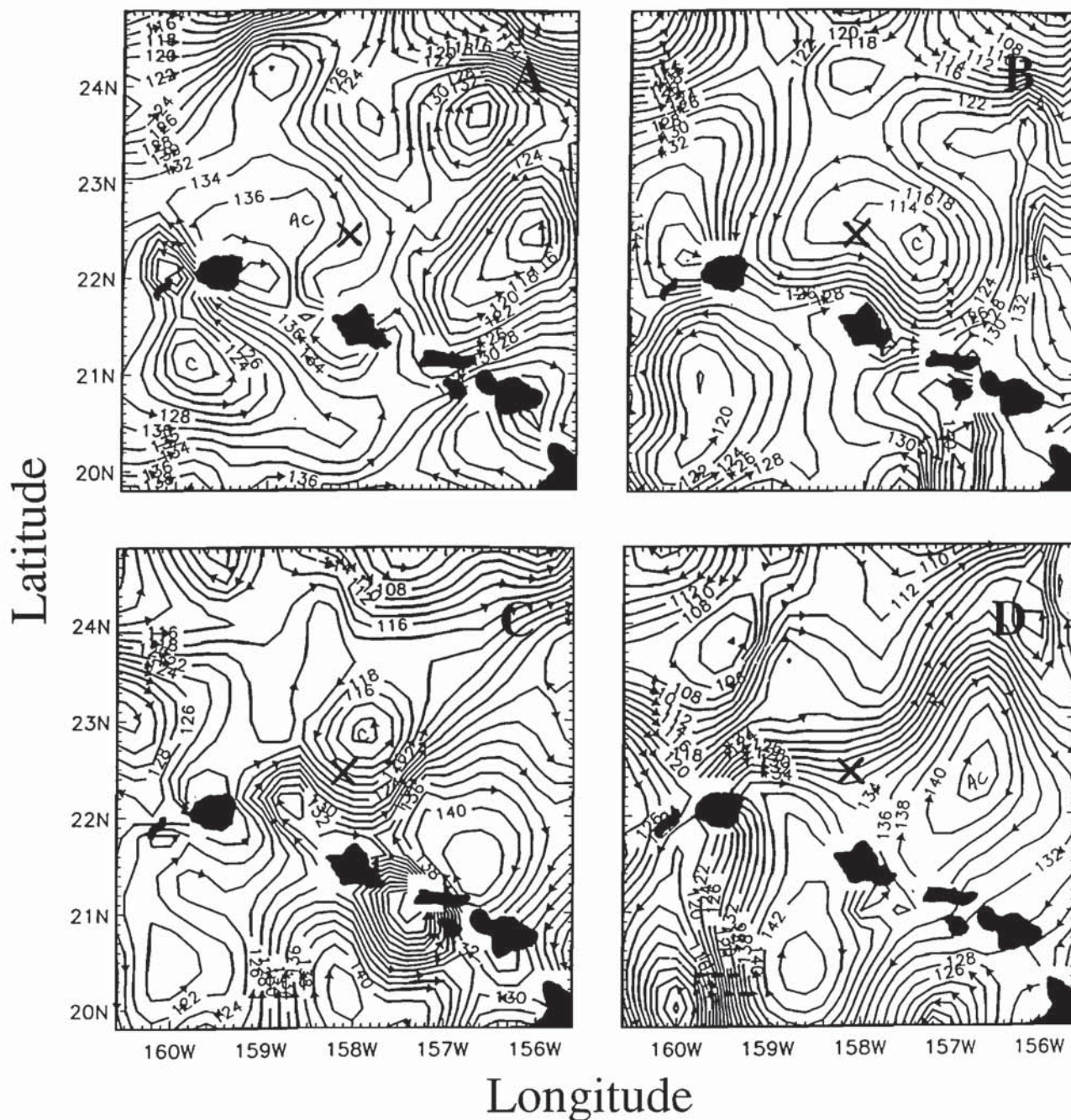


**Figure 4.** Temporal evolution of the sea surface anomaly calculated using TOPEX/ERS 2 and AVISO: (a) February 28, (b) March 20, (c) April 9, and (d) April 24. (Contour units are centimeters.)

the premature demise of the Advanced Earth Observing Satellite (ADEOS) on June 30, 1997.

#### 4.1. Upper Water Column (0–25 m) Temporal Evolution

Based on the moored temperature and optical records, it is possible to detect at least two distinct temporal scales of response for the phytoplankton community triggered by the passage of the cyclonic eddy. The first response is an increase in CFE in the upper portion (0–25 m) of the water column, coincident with the sudden shoaling of the thermocline. The second response is an

increase in chl *a* concentrations. A significant lag period (1 week) exists between the recorded maximum CFE and the observed change in chl *a*.

The absence of an increase of chl *a* concentration in the upper euphotic zone at the onset of the upwelling suggests that, although a strong upward vertical displacement occurred initially, it was not sufficient to mix the DCML into the upper 25 m of the water column. Alternatively, this lack of a detectable change in chl *a* concentration following the DCML displacement could indicate that phytoplankton photoadaptation kept pace with the rate of change of the light field perceived by the phytoplankton

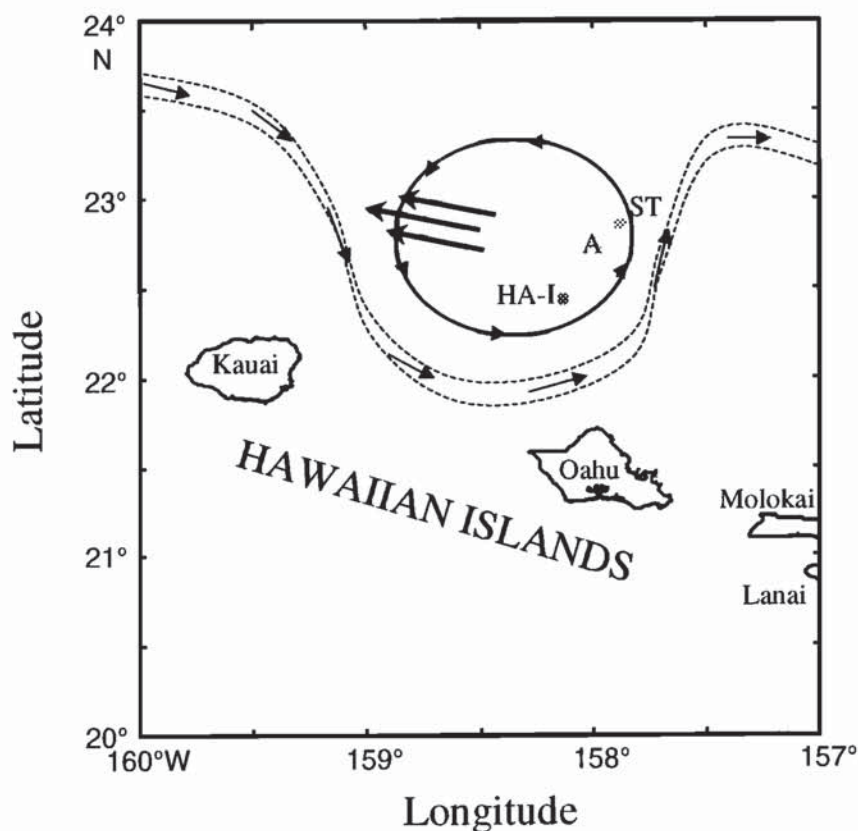


**Figure 5.** Schematic diagram displaying the displacement of the cyclonic eddy relative to the meandering of the zonal front (A, Station ALOHA; HA-I, HALE ALOHA; ST, deep moored sediment traps).

community [Denman and Marra, 1986; Cullen and Lewis, 1988]. Based on the observed mean cruise position of the DCML during HOT-80 (120 m, Figure 8a) and the vertical displacement of isotherms recorded between HOT-80 and HOT-81 (e.g., the 23°C isotherm, Plate 1a) we calculate that the DCML may have risen to

a depth of 50 m on March 7. The strong CFE signal detected during this period suggests that phytoplankton brought into the surface layer did not have time for photoadaptation to the rapid change in light regime (Figure 2).

Variations in photosynthesis and fluorescence quantum yield

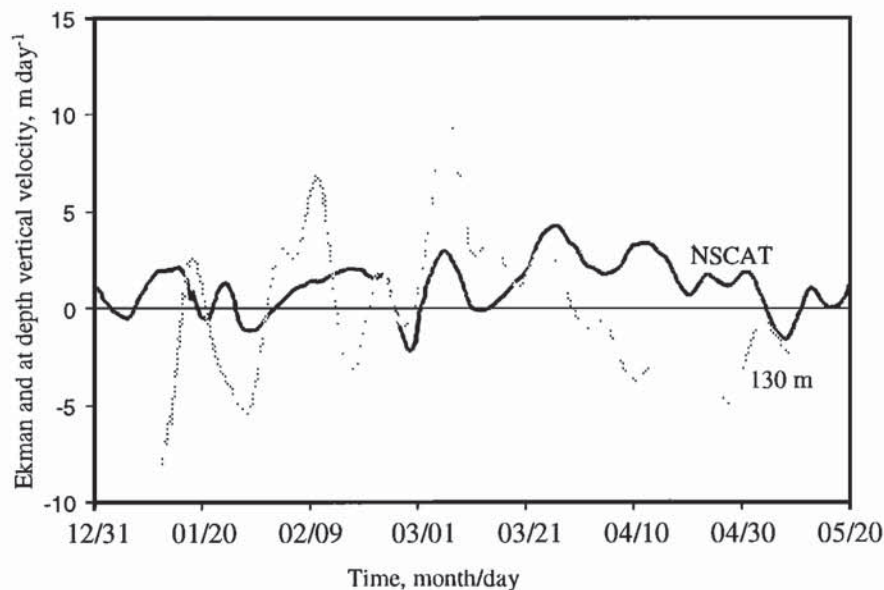


**Figure 6.** Time series of Ekman pumping velocity and water column vertical velocity at 130 m depth derived from NSCAT wind scatterometry and moored temperature data, respectively.

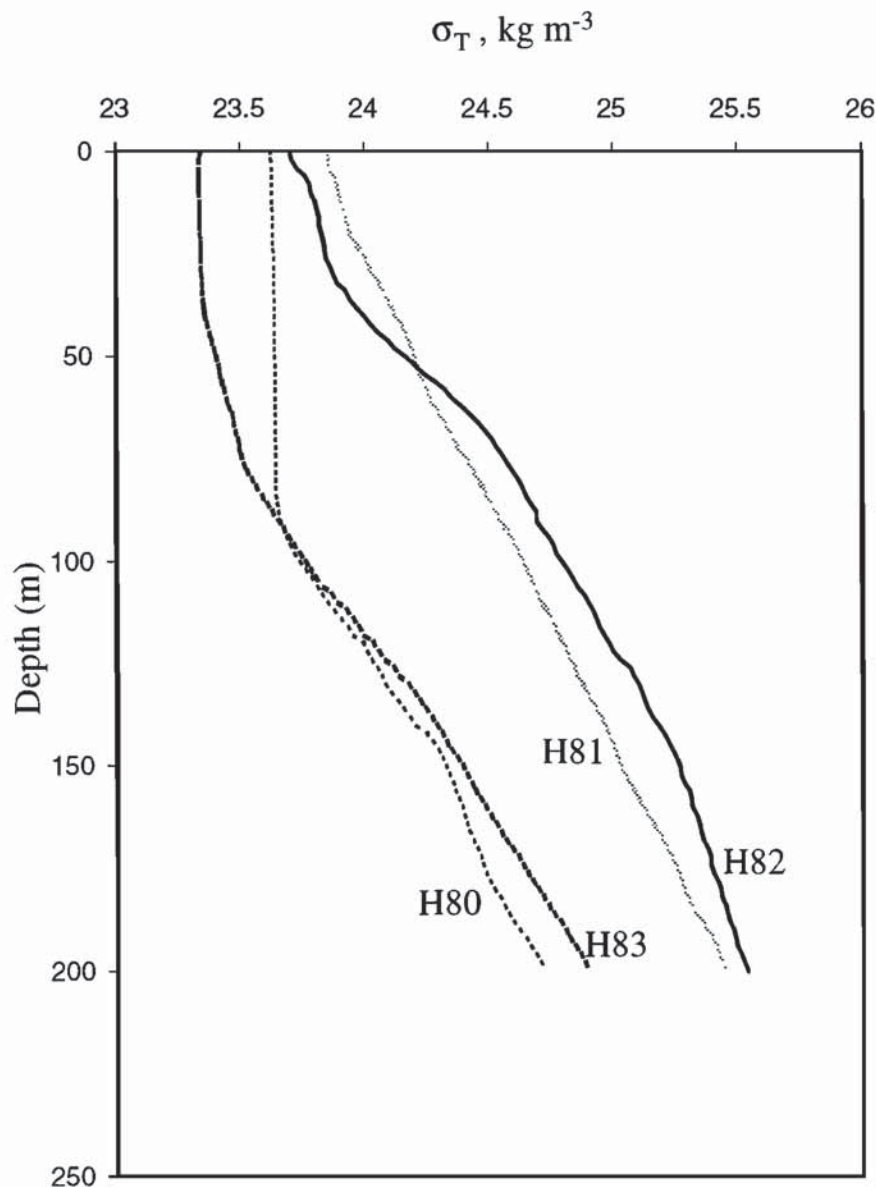
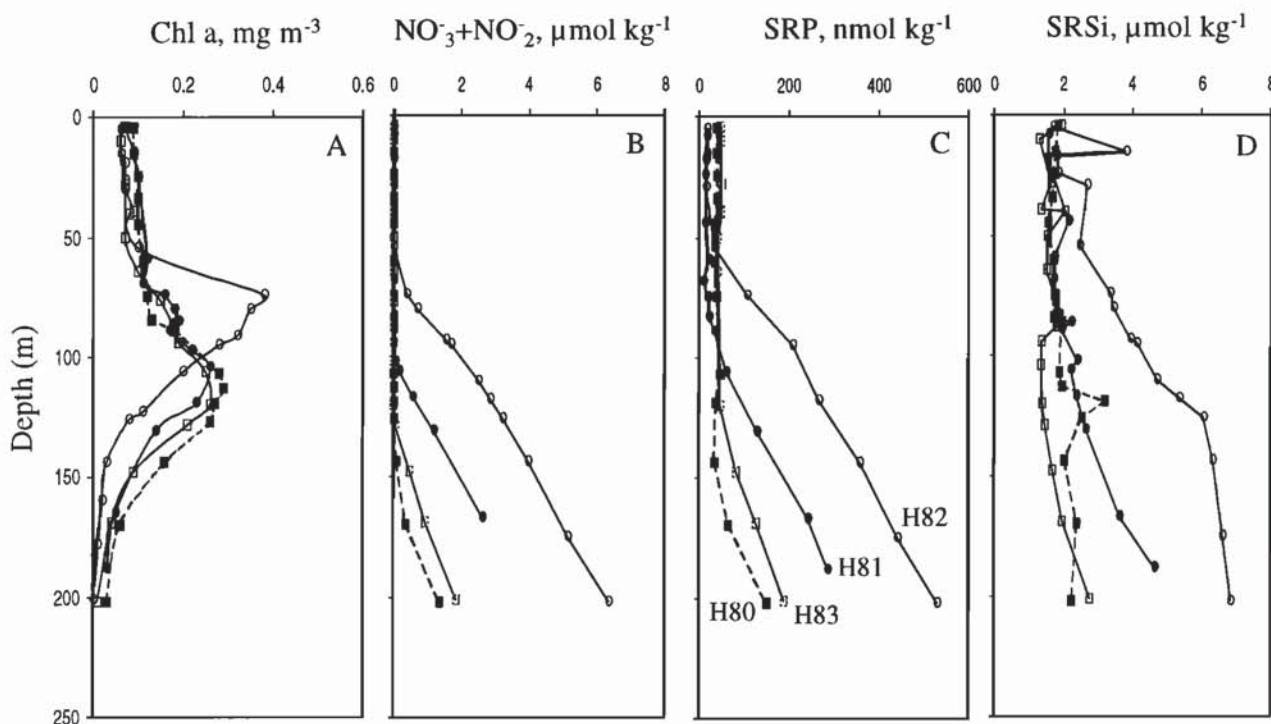


Figure 7. Mean depth distribution of  $\sigma_T$  recorded during cruises HOT-80 through HOT-83.

( $\Phi_p$  and  $\Phi_f$ , respectively) arise when the fraction of radiant energy absorbed by the photosystem and used in photosynthesis is changed. These changes are mainly the result of variations in nutrient availability, light regime and phytoplankton species composition [Geider *et al.*, 1993]. The first increase in CFE observed in the HALE ALOHA-I record corresponds to the sudden rise of the thermocline and may indicate phytoplankton physiological stress resulting from an increase in photosynthetically available radiation (PAR). If photosynthetic rates are controlled by the capacity of the Calvin cycle under nutrient limiting conditions [Behrenfeld *et al.*, 1998], phytoplankton cells experiencing an increase in PAR without a concomitant change in nutrient availability may initially increase the amount of radiation absorbed by the photosystem without increasing the rates of carbon fixation. Under this scenario the probability of energy dissipation within the photosystem as fluorescence and heat increases [Kiefer and Reynolds, 1992].

Although it is not possible with the available data set to assess the role of a change in species composition in this first CFE signal, it is nevertheless possible to discard an initial change in nutrient availability. An influx of nutrients to the upper euphotic zone relieving phytoplankton nutrient limitation would have increased  $\Phi_p$  with an inverse effect on  $\Phi_f$ , which was not observed. Furthermore, the same rationale used to estimate the shoaling of the DCML suggests that the initial vertical displacement of isotherms brought the nutricline to approximately 60 m depth, while the spectroradiometer only detected changes in the upper 25 m.

Both the increases in CFE and CDOM, which started on March 5, are independent signals indicating that a parcel of water was displaced from a light-shaded region of the water column into a region with significantly higher light levels. In the upper euphotic zone of oligotrophic pelagic environments, photobleaching decreases the CDOM concentration [Nelson *et*



**Figure 8.** Mean depth distribution of (a) chlorophyll *a*, (b)  $[\text{NO}_3 + \text{NO}_2]$ , (c) soluble reactive phosphorus [SRP], and (d) soluble reactive silicate [SRSi], recorded during cruises HOT-80 through HOT-83.

*al.*, 1998]. Although DOM distribution does not necessarily follow the same depth pattern as CDOM, changes in CDOM at a specific depth stratum or isolume may prove to be useful a indicator of variations in the vertical velocity of water within the euphotic zone. While the relative increase in CDOM is coupled to the upwelling period, the sudden decrease in CDOM beginning on March 28 (Figure 2) coincides with onset of the deepening of isotherms recorded by the mooring thermistor array. The CDOM signal remains depressed during most of the subsequent downwelling period.

Even though both signals (CFE and CDOM) increase concurrently, CFE declines several days before a significant decrease in CDOM is detected. While the decrease in CDOM appears to be caused by the onset of a downwelling period, the most probable mechanism to explain the premature decline in CFE is a relaxation of phytoplankton nutrient limitation in the upper 25 m of the water column. This nutrient relaxation also explains the increase in chl *a* concentrations observed a few days later (Figure 2). When placed in the full context of the HOT record, the estimated 0–25 m chl *a* increase is the largest reported to date, with the exception of a *Trichodesmium* spp. bloom sampled in August 1989 [Karl *et al.*, 1992]. Assuming a conversion factor of 47 g C per g chl *a* for mixed layer winter phytoplankton in the North Pacific Subtropical Gyre [Letelier *et al.*, 1993], the observed change in the 0–25 m chl *a* concentration corresponds to an net increase of 225 mg C m<sup>-2</sup> in phytoplankton carbon stock. Even though the absolute magnitude of this change represents on average only 8 days of 150 m exported particulate carbon flux at Station ALOHA, as measured by free-drifting sediment traps [Karl *et al.*, 1996], the estimated augmentation of particulate matter and chl *a* may have important short-term effects on the ecosystem and elemental fluxes. For example, the increase in chl *a* close to the surface suggests an enhancement of

gross productivity with the concomitant increase of energy available to higher trophic levels. Furthermore, a larger phytoplankton biomass in ocean surface will alter the light field below, inducing an environmental shift for the full water column phytoplankton assemblage and, perhaps, migrating mesozooplankton as well.

Although the moored time series record of temperature indicates that the top of the nitracline did not reach the upper 25 m of the water column, it may be possible to attribute the injection of nutrients to the spatial heterogeneity within the cyclonic feature or to other small-scale mixing processes near the top of the nitracline. Changes in nutrient concentration could also explain the secondary CFE maximum recorded during mid April. This signal could have been triggered by the depletion of nutrients following the increase in phytoplankton biomass during late March and early April [Geider *et al.*, 1993; Letelier *et al.*, 1997].

Samples collected as part of the four HOT cruises covering the February–May 1997 period (HOT-80 through HOT-84) also display the doming of the density field as a result of the cyclonic feature (Figure 7). However, there is no indication of a significant increase in chlorophyll concentration in the upper water column during this period. The mooring optical record suggests that the HOT-81 and HOT-82 cruises took place just before and just after, respectively, the high chl *a* concentrations were recorded in the upper 25 m, effectively missing this signal. However, the analysis of the relative abundance of phytoplankton pigments during these cruises indicates that the algal assemblage in the upper euphotic zone within the eddy had distinct characteristics.

The observed relative increase in fucoxanthin (Table 2) suggests that the microbial assemblage sampled during March and April (HOT-81 and HOT-82, respectively) had twice the

**Table 2.** Comparison of HPLC Pigment and Inorganic Nutrient Concentrations in the Upper 25 m of the Water Column of Station ALOHA Based on HOT Program Measurements Made Between February and May 1997

| Parameters  | Cruise Number, Cruise Date |                     |                    |                   |                       |
|---|----------------------------|---------------------|--------------------|-------------------|-----------------------|
|   | HOT-80<br>Feb 16-20        | HOT-81<br>Mar 10-14 | HOT-82<br>Apr 7-11 | HOT-83<br>May 5-9 | HOT 1-79<br>1988-1997 |
| Number of samples   | 2                          | 2                   | 2                  | 1                 | >55                   |
| Chl <i>a</i> , $\mu\text{g m}^{-3}$                           | 87.5 (1.0)                 | 91.0 (17.7)         | 74.5 (19)          | 73.2              | 75.1 (0.5)            |
| Chl <i>b</i> , $\mu\text{g m}^{-3}$                           | 8.0 (0.04)                 | 8.5 (3.0)           | 4.0 (2.3)          | 6.0               | 5.3 (1.4)             |
| Fucoxanthin, $\mu\text{g m}^{-3}$                             | 3.5 (1.0)                  | 8.0 (2.2)           | 7.5 (0.9)          | 3.9               | 6.3 (1.1)             |
| Zeaxanthin, $\mu\text{g m}^{-3}$                              | 53.0 (3.9)                 | 84.0 (6.0)          | 65.0 (1.2)         | 61.2              | 50.7 (0.6)            |
| Fucoxanthin:chl <i>a</i>                                      | 0.04                       | 0.09                | 0.10               | 0.05              | 0.08 (0.02)           |
| Number of samples   | 3                          | 2                   | 4                  | 3                 | >54                   |
| [NO <sub>3</sub> + NO <sub>2</sub> ], $\mu\text{mol kg}^{-1}$ | 0.5 (0.5)                  | 0.7 (0.1)           | 1.2 (0.2)          | 0.8 (0.1)         | 3.7 (3.3)             |
| [PO <sub>4</sub> ], $\text{nmol kg}^{-1}$                     | 38.1 (1.0)                 | 14.6 (2.7)          | 16.0 (0.1)         | 48.0 (1.5)        | 68.0 (1.7)            |
| [SiO <sub>4</sub> ], $\mu\text{mol kg}^{-1}$                  | 1.52 (0.07)                | 1.5 (0.09)          | 1.38 (0.03)        | 1.70 (0.34)       | 1.30 (1.76)           |

Values are expressed as mean (standard deviation) for sample size > 2 and as mean (range) for sample size = 2.

concentration of diatoms observed in the assemblages sampled during February and May (HOT-80 and HOT-83, respectively). Because diatoms are a minor component of the algal standing stock in terms of their contribution to total chl *a* at Station ALOHA, typically accounting for < 1% of the total chl *a* standing stock [Ondrusek et al., 1991; Letelier et al., 1993; Andersen et al., 1996], a doubling in their biomass may not change significantly the total phytoplankton biomass. However, diatoms are implicated in the control of new and exported production processes [Legendre and Lefèvre, 1989; Dugdale and Wilkerson, 1998; Scharek et al., 1999]. Hence, even subtle transient shifts in microbial community composition may have had a significant impact in nutrient and carbon cycles within the euphotic zone. Furthermore, assuming that the ratio of fucoxanthin to chl *a* in the upper euphotic zone remained constant between HOT-81 and HOT-82, the threefold increase in chl *a* recorded by the mooring between these cruises translates into a sixfold increase in diatom biomass inside the eddy. Nevertheless, by May 1997 all signs of a shift in the phytoplankton community structure had disappeared. HOT sediment trap records have documented the increase in export production rates during late winter [Karl et al., 1996]. The isotopic nitrogen signature ( $\delta^{15}\text{N}$ ) indicates that this export is the result of an increase in nitrate within the euphotic zone [Karl et al., 1997].

#### 4.2. Temporal Evolution of Water Column Profiles

The temporal evolution of chl *a* and nutrient profiles derived from shipboard measurements collected during the mooring deployment period display two striking features when analyzed in the context of the evolution of the water column density structure. One of these features is the apparent absence of a change in the magnitude or position of the deep chlorophyll maximum layer (DCML) during HOT-81 (Figure 8a). Although this profile was collected only 5 days following the initial large vertical displacement recorded by the mooring, there are no signs of an effect of this vertical displacement on the depth distribution of chl *a*. One possible explanation for this observation is the presence of spatial heterogeneity in the depth distribution of properties within the eddy and the fact that the HALE ALOHA mooring site is located approximately 37 km south of Station ALOHA (Figure

1). However, chl *a* profiles collected at Station ALOHA and at HALE ALOHA-I during HOT-81 do not display significant differences in their depth structure; both profiles have the DCML located at approximately 105 m depth and a mean 0-25 m chl *a* concentration close to  $0.09 \text{ mg m}^{-3}$ . Furthermore, the density structure and the position of the nutricline recorded during HOT-81 suggest that this cruise sampled an area in which the water column had already been vertically displaced.

The one mechanism to explain the apparent stability of the DCML depth location and magnitude is based on the kinetics of phytoplankton photoadaptation observed in cells grown under nutrient-sufficient growth conditions. Cullen and Lewis [1988] estimated that under nutrient sufficient conditions the rates of photoadaptation in *Thalassiosira pseudonana* ranged on the order of hours to 1 day. Although these observations appear to contradict the conclusions derived previously from the dynamics of CFE in the upper 25 m of the water column, the discrepancy may be due to the role that nutrient limitation plays in the physiological response of phytoplankton to strong increase of PAR. While changes in CFE recorded by the spectroradiometer indicate alterations in the energy distribution within the photosystem resulting from an increase in the light field under nutrient-limiting conditions (upward displacement of the water column without the intrusion of the top of the nutricline into the mixed layer), the mean position of the DCML is regulated by the production and degradation of chl *a* as a response to the light distribution within the euphotic zone. Hence the lack of a detectable change in the relative depth distribution of chl *a* between HOT-81 and HOT 82 suggests that the light depth penetration was not significantly affected between cruises.

A second enigmatic feature is the evolution of the nutricline depth distribution relative to that of the pycnocline. The main shoaling of the pycnocline took place between HOT-80 and HOT-81 (February 16-20 and March 10-14, respectively; Figure 7). There was only a small displacement (approximately 5 to 10 m) between HOT-81 and HOT-82 (April 7-11), followed by a deepening observed during HOT-83 (May 5-9). This temporal evolution is confirmed by the HALE ALOHA-I thermistor record (Plate 1a). However, when the depth position of the nutricline is analyzed, we observe a continuous and significant rising between HOT-80 and HOT-82 (an upward displacement of approximately

**Table 3.** Comparison of Nutrient Concentration Variability in the Upper Water Column Based on a Fixed Depth Interval (0–100 m) and Fixed Percentage Surface Light Level Depth (100–1%  $E_{d443}$ ) Integrations

| Parameters  | Cruise Number |        |        |        |
|---|---------------|--------|--------|--------|
|   | HOT-80        | HOT-81 | HOT-82 | HOT-83 |
| 0–100 m   |               |        |        |        |
| [NO <sub>3</sub> + NO <sub>2</sub> ] ( $\mu\text{mol m}^{-2}$ ) | 68            | 47     | 27,370 | 96     |
| [PO <sub>4</sub> ] ( $\mu\text{mol m}^{-2}$ )                   | 3.84          | 1.87   | 5.80   | 4.34   |
| 100–1% $E_{d443}$   |               |        |        |        |
| 1% $E_{d443}$ depth (m)   | 104           | 112    | 73     | 103    |
| [NO <sub>3</sub> + NO <sub>2</sub> ] ( $\mu\text{mol m}^{-2}$ ) | 72            | 120    | 81     | 98     |
| [PO <sub>4</sub> ] ( $\mu\text{mol m}^{-2}$ )                   | 4.12          | 2.36   | 2.44   | 4.83   |

65 m between HOT-80 and HOT-81 followed by another 45 m displacement between HOT-81 and HOT-82; Figure 8b–d). If we integrate the dissolved inorganic nitrogen pool in the upper 100 m of the water column as a lower bound on the nitrate introduced into the euphotic zone, we conclude that most of the nitrate was injected between March and April (Table 3). Furthermore, the depth distribution of chl *a* during April (HOT-82) also displays a significant shoaling of the DCML (Figure 8a).

The short-term variability (less than a day) of the DCML position is controlled by the vertical displacements of the water column, resulting from internal waves, tidal forcing, and near inertial period oscillations. However, its calculated mean depth during a given cruise (once the short-term variability has been removed) is controlled by the previous light history and nutrient distribution in the upper water column [Letelier *et al.*, 1993]. HOT-82 took place following a period of increasing surface chl *a*, as indicated by the moored optical sensor record. Although it is not possible to reconstruct the full water column light field prior to each cruise from the data that are available, it is nevertheless possible to estimate the effect that the temporal distribution of the 0–25 m chl *a* and CDOM have on the light attenuation based on the spectroradiometer data.

To calculate the maximum depth of the 1% light level at different wavelengths we used the light attenuation coefficient for pure water at 412, 443, 490, and 555 nm published by Smith and Baker [1981]. In this model calculation, we assume that changes in chl *a* and CDOM concentrations do not affect significantly the total attenuation at 555 nm and that the sea surface light spectrum between 412 and 555 nm is flat (i.e., the photon flux at any wavelength within this interval is not significantly different from the photon flux measured at 555 nm). Hence changes in the irradiance ratio between a selected wavelength *X* (where 412 nm  $\leq X < 555$  nm) and 555 nm will be predominantly the result of a change in the attenuation coefficient at wavelength *X*.

Based on these calculations, we estimated that the mean 1% light level depths for 412, 443 and 490 nm during the period between January 20 and March 1, 1997 were 84, 104, and 105 m, respectively. However, the extinction of light increased significantly between March 21 and April 20 attaining 1% light level depths as shallow as 64 m for  $E_{d443}$  and 76 m for  $E_{d490}$ .

To assess the light history of the water column affecting phytoplankton distribution prior to each cruise, we calculated the mean light attenuation coefficient at 443 nm for the preceding 7 days. We used 443 nm in this calculation because the maximum absorption of naturally occurring phytoplankton assemblages in oligotrophic region is centered around this wavelength [Iturriaga and Siegel, 1989].

When chl *a* and nutrient depth distributions are plotted as functions of light history, the DCML for all cruises fall around the 1% light level (Figure 9a), and two distinct distributions are observed for the nutricline (Figure 9b). While the top of the nitracline for HOT-80 and HOT-83 is positioned at the approximately 0.2% level, it rises to approximately 1% light level in the profiles collected inside the eddy (HOT-81 and HOT-82). However, it is difficult to assess the significance of the differences between these profiles. Our calculations of light attenuation do not consider the effect that the DCML has on the light field in the lower regions of the euphotic zone. Furthermore, changes in the concentrations of chl *a* at the base of the euphotic zone are not necessarily correlated to those observed in the surface [Letelier *et al.*, 1993; Winn *et al.*, 1995]. Nevertheless, both the mean position of the DCML and of the depth of the nutricline observed during HOT-82 strongly suggest that the depth of the euphotic zone decreased significantly as a result of the upwelling event.

Two tentative conclusions can be derived from the analysis of the CDOM and chl *a* shading effect. The first conclusion is that, although the initial shoaling of the nutricline between HOT-80 and HOT-81 was probably the result of physical advection, the subsequent displacement (between HOT-81 and HOT-82) can be attributed to a reduction in nutrient photoautotrophic nutrient uptake at depth. This reduction is the consequence of a decrease in PAR at depth (Figure 9) caused by an increase in chl *a* and CDOM concentrations in the upper water column.

The second conclusion is in reference to the calculation of nutrient injections into the euphotic zone. If instead of integrating the concentration of nutrients over a fixed depth range we use a depth range defined by an isolume, then the temporal variation of nutrient availability for phytoplankton will display a different pattern for the period comprising HOT-80 through HOT-83 (Table 3). For example, no significant differences are observed between cruises when nutrients are integrated to the 1% light level depth. Hence estimates of phytoplankton nutrient availability based on variations of the nutrient depth distribution must take into account the evolution of the light field resulting from temporal changes in phytoplankton biomass. In general, present models estimating nitrate injections into the euphotic zone as a consequence of eddy activity assume a fixed euphotic zone depth [McGillicuddy and Robinson, 1997; Oschlies and Garçon, 1998].

#### 4.3. A HOT Perspective

Both recurrent short-term perturbations and long-term gradual environmental changes are important forces shaping the

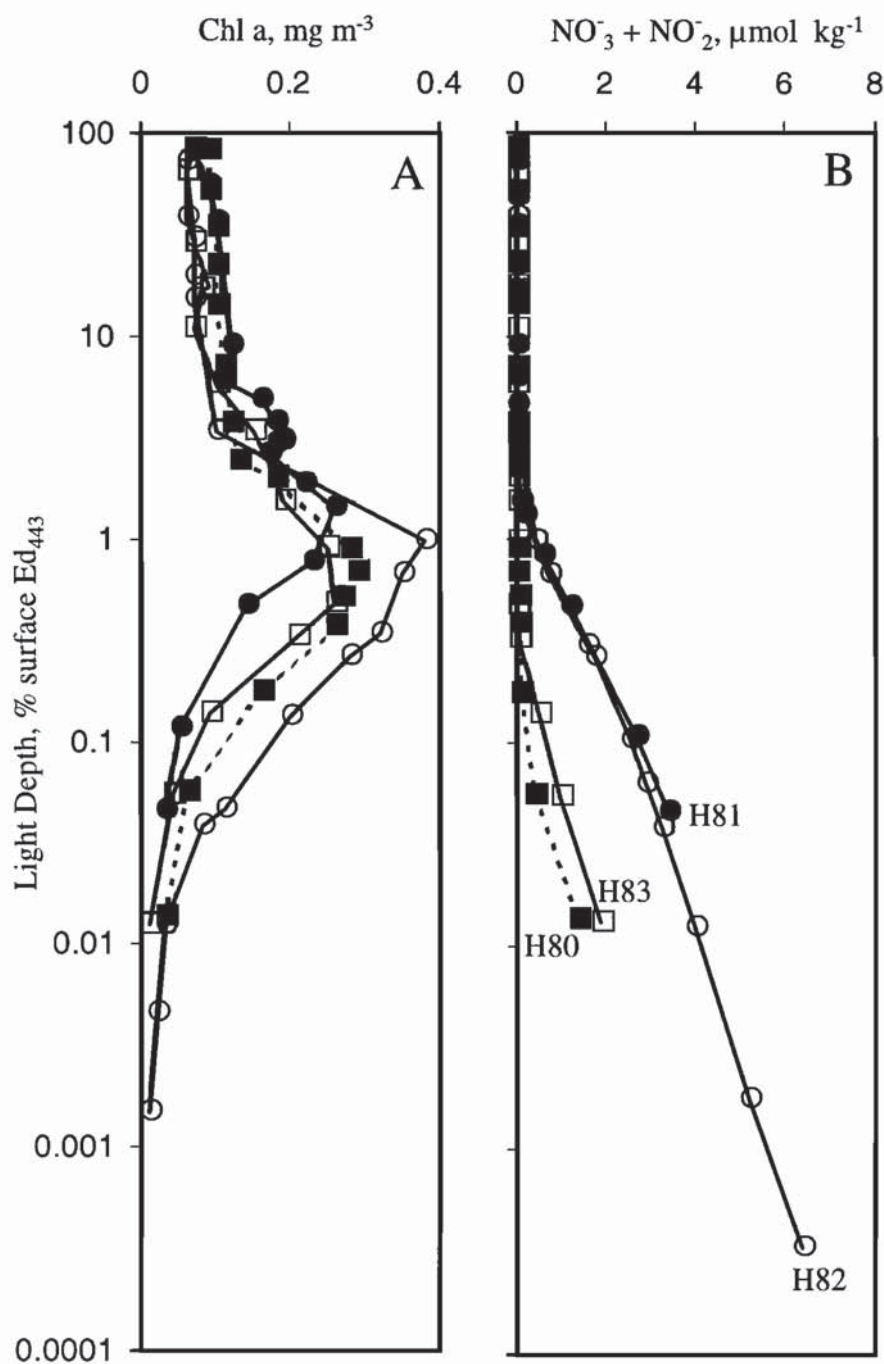


**Figure 9.** Distribution of (a) chlorophyll and (b)  $[\text{NO}_3^- + \text{NO}_2^-]$ , as a function of the percentage of surface irradiance at 443 nm.

ecosystem structure. In this context the results generated by the HOT program over the past decade display temporal variability at all scales of resolution (from subseasonal through interannual variability). This is particularly clear when analyzing the time series of 0–100 m nutrient availability derived from the cruise records [Karl *et al.*, 1996; Karl, 1999]. Although month-to-month variability is significant during all times of the year, large nutrient injections into the upper 100 m are usually recorded as single cruise events during late winter. The recorded magnitude of these nutrient winter events also varies dramatically from year-to-year, ranging from being absent during some years to 27 mmol

$[\text{NO}_3^- + \text{NO}_2^-] \text{ m}^{-2}$  during April 1997 (the mean value for the first 9-year 0–100 m HOT record is  $0.4 \mu\text{mol m}^{-2}$  [Karl, 1999]).

Our analysis of the integration of several independent time series records indicates that the ecological interpretation of these winter pulse nutrient events is not straightforward. Different mechanisms, such as storm-induced mixing [DiTullio and Laws, 1991], breaking of internal waves [McGowan and Hayward, 1978], eddy-induced upwelling [Allen *et al.*, 1996], Ekman pumping and light availability (this study) may all play important roles in the observed increase in upper water column nutrient availability. However, pelagic communities will respond

differently to each of these forces. Based only on the cruise information, it is not possible to assess the extent to which the sporadic shoaling of the nutricline is the result of physical upwelling. The shoaling of isolines caused either by physical factors such as overcast skies or the passage of clouds [Banse, 1987], or biological factors such as the increase in pigments in the surface layers (this study) may play a role of greater importance than previously thought in the observed depth variability of the nutricline between cruises. However, upwelling nutrient injection and displacement of isolines will have different effects on the pelagic community structure and function. Furthermore, nutrients displaced upward into the base of the euphotic zone will be utilized by photoautotrophs if they remain in an environment with sufficient light. A significant deepening of the thermocline, such as the one observed following HOT-82, may limit the biological utilization of these nutrients.

Several conclusions can be derived from the HOT program observations regarding these wintertime nutrient pulses: (1) their duration is short lived (< 2 month), (2) they produce or are the product of significant physicochemical changes at the base of the euphotic zone, and (3) they can have a profound effect on local and regional plankton processes. In regions like the North Pacific Subtropical Gyre where seasonal cycles generally do not dominate the frequency spectrum of variability [Cushing, 1959; Winn *et al.*, 1995], the interannual or longer-term variability in the frequency of nutrient-pulsed events may be a critical factor in shaping the community structure and biogeochemical cycles. For example, Karl *et al.* [1995, 1997] and Letelier and Karl [1996] noted that the reduction in mixed-layer depth variability and the absence of detectable winter-nutrient pulses during 1991 and 1992 was accompanied by the proliferation of diazotrophs and a shift from nitrogen to phosphorus limitation in the pelagic ecosystem.

In this context, the pulsed ecosystem paradigm [e.g., Odum *et al.*, 1995], in which the interaction of internal and external pulses reinforces the system's characteristics, seems to be applicable to the North Pacific Subtropical Gyre ecosystem [Karl, 1999]. If this is the general case for pelagic ecosystems with low amplitude seasonal variability, it will be difficult to characterize and evaluate the mean effect that the community has on the biogeochemical cycles unless we also include the characterization of its perturbation scales [Harris, 1980, 1986; Legendre and Demers, 1984].

The interdisciplinary time series data sets available through the deployment of HALE ALOHA provide continuous observations that are critical for the interpretation of the biogeochemical changes observed during the approximately monthly ship-based core measurement program. The availability of two-dimensional maps, derived from satellite observations, further enhances our capacity for interpretation by providing evidence of the mechanisms generating fourth-dimension mesoscale variability. Together, these otherwise disparate data sets are providing important clues to help us understand the main forces controlling the ecosystem structure in the North Pacific Subtropical Gyre.

**Acknowledgments.** We are indebted to the Captains, crew and scientists responsible for the monthly sampling and characterization of the water column properties at Station ALOHA, especially T. Houlihan and K. Björkman (high-sensitivity nutrients), D. Sadler (fluorometric chl *a*), and R. Bidigare (HPLC pigments). We also thank T. Houlihan, D. Young, M. Sawyer, and H. Ramm for their contributions to the HALE ALOHA-I experiment and C. James for the processing of the TOPEX/ERS 2 data. Jeffrey Polovina, Jasmine Bartlett, Andrew Dickson,

and two anonymous reviewers gave valuable comments that helped improve the present manuscript. The present research was funded by NSF grants OCE 93-03094 (to Roger Lukas), OCE 93-01368 (to David M. Karl), OCE 96-01850 (to David Karl, Roger Lukas, and Pierre Flament) and NASA grant NAGW-4596 (to Mark R. Abbott). SOEST publication 5264 and U.S. JGOFS publication 581.

## References

- Abbott, M. R., and R. M. Letelier, Decorrelation scales of chlorophyll as observed from bio-optical drifters in the California Current, *Deep Sea Res.*, **45**, 1639-1668, 1998.
- Allen, C. B., J. Kana, and E. A. Laws, New production and photosynthetic rates within and outside a cyclonic mesoscale eddy in the North Pacific Subtropical Gyre, *Deep Sea Res.*, **43**, 917-936, 1996.
- Andersen, R. A., R. R. Bidigare, M. D. Keller, and M. Latasa, A comparison of HPLC pigment signatures and electron microscopic observations for oligotrophic waters of the North Atlantic and Pacific Oceans, *Deep Sea Res.*, **43**, 517-537, 1996.
- Angel, M. V., and M. J. R. Fasham, Eddies and biological systems, in *Eddies in Marine Systems*, edited by A. R. Robinson, pp. 492-524, Springer-Verlag, New York, 1983.
- Banase, K., Clouds, deep chlorophyll maxima and the nutrient supply to the mixed layer of stratified water bodies, *J. Plankton Res.*, **9**, 1031-1036, 1987.
- Behrenfeld, M. J., O. Prasil, Z. S. Kolber, M. Babín, and P. G. Falkowski, Compensatory changes in photosystem II electron turnover rates protect photosynthesis from photoinhibition, *Photosynthesis Res.*, **58**, 259-268, 1998.
- Carder, K. L., S. K. Hawes, K. A. Baker, R. S. Smith, R. G. Steward, and B. G. Mitchell, Reflectance model for quantifying chlorophyll *a* in the presence of productivity degradation products, *J. Geophys. Res.*, **96**, 20,599-20,611, 1991.
- Chiswell, S. M., Intra-annual oscillations at Sta. ALOHA, north Oahu, Hawaii, *Deep Sea Res.*, **43**, 305-319, 1996.
- Clark, D. K., Phytoplankton pigment algorithm for the Nimbus-7 CZCS, in *Oceanography from Space*, edited by J. F. R. Gower, pp. 227-238, Plenum, New York, 1981.
- Cullen, J. J., and M. R. Lewis, The kinetics of algal photoadaptation in the context of vertical mixing, *J. Plankton Res.*, **5**, 1039-1063, 1988.
- Cushing, J. D., The seasonal variation in oceanic production as a problem in population dynamics, *J. Cons. Int. Explor. Mer.*, **24**, 455-464, 1959.
- Dayton, P. K., and M. J. Tegner, The importance of scale in community ecology: A kelp forest example with terrestrial analogs, in *A New Ecology: Novel Approaches to Interactive Systems*, edited by P. W. Price, C. M. Slobodkin, and S. W. Gaud, pp. 457-481, John Wiley, New York, 1984.
- DeAngelis, D. L., *Dynamics of Nutrient Cycling and Food Webs*, 270 pp., Chapman and Hall, New York, 1992.
- Denman, K. L., A time-dependent model of the upper ocean, *J. Phys. Oceanogr.*, **3**, 173-184, 1973.
- Denman, K. L., and J. Marra, Modelling the time dependent photoadaptation of phytoplankton to fluctuating light, in *Marine Interface Ecohydrodynamics*, edited by J. C. J. Nihoul, pp. 341-359, Elsevier Sci., New York, 1986.
- Dickey, T., The emergence of high-resolution physical and bio-optical measurements in the upper ocean and their applications, *Rev. Geophys.*, **29**, 383-413, 1991.
- DiTullio, G. R., and E. A. Laws, Impact of an atmospheric-oceanic disturbance on phytoplankton community dynamics in the North Pacific central gyre, *Deep Sea Res.*, **38**, 1305-1329, 1991.
- Dore, J. E., and D. M. Karl, Nitrite distributions and dynamics at Station ALOHA, *Deep Sea Res.*, **43**, 385-402, 1996.
- Dugdale, R. C., and J. J. Goering, Uptake of new and regenerated forms of nitrogen in primary productivity, *Limnol. Oceanogr.*, **12**, 196-206, 1967.
- Dugdale, R. C., and F. P. Wilkerson, Silicate regulation of new production in the Equatorial Pacific upwelling, *Nature*, **391**, 270-273, 1998.
- Falkowski, P. G., D. Ziemann, Z. Kolber, and P. K. Bienfang, Role of eddy pumping in enhancing primary production in the ocean, *Nature*, **352**, 53-58, 1991.
- Falkowski, P. G., R. T. Barber, and V. Smetacek, Biogeochemical controls and feedbacks on ocean primary production, *Science*, **281**, 200-206, 1998.

- Franks, P. J. S., J. S. Wroblewski, and G. R. Flierl, Prediction of phytoplankton growth in response to the frictional decay of a warm-core ring, *J. Geophys. Res.*, **91**, 7603-7610, 1986.
- Freilich, M. H., ERS-1 scatterometer measurements over the Southern Ocean, in *Proceedings of the Second ERS-1 Symposium*, Eur. Space Agency Spec. Publ., ESA SP-361, 1111-1115, 1994.
- Garside, C., A chemiluminescent technique for the determination of nanomolar concentration of nitrate and nitrite in seawater, *Mar. Chem.*, **11**, 159-167, 1982.
- Geider, R. J., J. La Roche, R. M. Greene, and M. Oliazola, Response of the photosynthetic apparatus of *Phaeodactylum tricornutum* (Bacillariophyceae) to nitrate, phosphate, and iron starvation, *J. Phycol.*, **29**, 755-766, 1993.
- Gill, A. E., *Atmosphere-Ocean Dynamics*, 662 pp., Academic, San Diego, Calif., 1982.
- Harris, G. P., Temporal and spatial scales in phytoplankton ecology: Mechanisms, methods and management, *Can. J. Fish. Aquat. Sci.*, **37**, 877-900, 1980.
- Harris, G. P., *Phytoplankton Ecology: Structure, Function and Fluctuation*, 386 pp., Chapman and Hall, New York, 1986.
- Hayward, T. L., The nutrient distribution and primary production in the Central North Pacific, *Deep Sea Res.*, **34**, 1593-1627, 1987.
- Hayward, T. L., Primary production in the North Pacific Central Gyre: A controversy with important implications, *Trends Ecol. Evol.*, **6**, 281-284, 1991.
- Iturriaga, R., and D. Siegel, Microphotometric characterization of phytoplankton and detrital absorption properties in the Sargasso Sea, *Limnol. Oceanogr.*, **34**, 1706-1716, 1989.
- Karl, D. M., A sea of change: Biogeochemical variability in the North Pacific subtropical gyre, *Ecosystems*, **2**, 181-214, 1999.
- Karl, D. M., and R. Lukas, The Hawaii Ocean Time-series (HOT) program: Background, rationale and field implementation, *Deep Sea Res.*, **43**, 129-156, 1996.
- Karl, D. M., and G. Tien, MAGIC: A sensitive and precise method for measuring dissolved phosphorus in aquatic environments, *Limnol. Oceanogr.*, **37**, 105-116, 1992.
- Karl, D. M., R. Letelier, D. V. Hebel, D. F. Bird, and C. D. Winn, *Trichodesmium* blooms and new nitrogen in the North Pacific gyre, in *Marine Pelagic Cyanobacteria: Trichodesmium and other Diazotrophs*, edited by E. J. Carpenter, D. G. Capone, and J. G. Rueter, pp. 219-237, Kluwer Acad., Norwell, Mass., 1992.
- Karl, D. M., R. Letelier, D. Hebel, L. Tupas, J. Dore, J. Christian, and C. Winn, Ecosystem changes in the North Pacific subtropical gyre attributed to the 1991-1992 El Niño, *Nature*, **373**, 230-234, 1995.
- Karl, D. M., J. R. Christian, J. E. Dore, D. V. Hebel, R. M. Letelier, and L. M. Tupas, Seasonal and interannual variability in primary productivity and particle flux at Station ALOHA, *Deep Sea Res.*, **43**, 539-568, 1996.
- Karl, D., R. Letelier, L. Tupas, J. Dore, J. Christian, and D. Hebel, The role of nitrogen fixation in biogeochemical cycling in the subtropical North Pacific Ocean, *Nature*, **388**, 533-538, 1997.
- Kiefer, D. A., and R. A. Reynolds, Advances in understanding phytoplankton fluorescence and photosynthesis, in *Primary Productivity and Biogeochemical Cycles in the Sea*, edited by P. G. Falkowski and A. D. Woodhead, pp. 155-174, Plenum, New York, 1992.
- Kirk, J. T. O., *Light and Photosynthesis in Aquatic Ecosystems*, 2<sup>nd</sup> Ed., 509 pp., Cambridge Univ. Press, New York, 1994.
- Krause, G. H., and E. Weis, Chlorophyll fluorescence and photosynthesis: The basics, *Annu. Rev. Plant Physiol. Plant Mol. Biol.*, **42**, 313-349, 1991.
- Krebs, C. J., *Ecology*, 800 pp., Harper Collins, New York, 80, 1985.
- Landry, M. R., et al., Iron and grazing constraints on primary production in the central equatorial Pacific: An EqPac synthesis, *Limnol. Oceanogr.*, **42**, 405-418, 1997.
- Latasa, M., M. R. Landry, L. Shluter, and R. R. Bidigare, Pigment specific growth and grazing rates of phytoplankton in the central equatorial Pacific, *Limnol. Oceanogr.*, **42**, 289-298, 1997.
- Laws, E., *Mathematical Methods for Oceanographers: An Introduction*, 343 pp., John Wiley, New York, 1997.
- Lawson, L. L., E. E. Hofmann, and Y. H. Spitz, Time series sampling and data assimilation in a simple marine ecosystem model, *Deep Sea Res.*, **43**, 625-651, 1996.
- Legendre, L., and S. Demers, Towards dynamical biological oceanography and limnology, *Can. J. Fish. Aquat. Sci.*, **41**, 2-19, 1984.
- Legendre, L., and J. Lefèvre, Hydrodynamical singularities as controls of recycled versus export production in oceans, in *Productivity of the Ocean: Present and Past*, edited by W. H. Berger, V. S. Smetacek, and G. Wefer, pp. 49-63, John Wiley, New York, 1989.
- Letelier, R. M. and D. M. Karl, The role of *Trichodesmium* spp. in the productivity of the subtropical North Pacific ocean, *Mar. Ecol. Prog. Ser.*, **133**, 263-273, 1996.
- Letelier, R. M., R. R. Bidigare, D. V. Hebel, M. Ondrusek, C. D. Winn, and D. M. Karl, Temporal variability of phytoplankton community structure based on pigment analysis, *Limnol. Oceanogr.*, **38**, 1420-1437, 1993.
- Letelier, R. M., J. E. Dore, C. D. Winn, and D. M. Karl, Seasonal and interannual variability in photosynthetic carbon assimilation at Station ALOHA, *Deep Sea Res.*, **43**, 467-490, 1996.
- Letelier, R. M., M. R. Abbott, and D. M. Karl, Chlorophyll natural fluorescence response to upwelling events in the Southern Ocean, *Geophys. Res. Lett.*, **24**, 409-412, 1997.
- Lewis, M. R., J. J. Cullen, and T. Platt, Phytoplankton and thermal structure in the upper ocean: Consequences of nonuniformity in chlorophyll profile, *J. Geophys. Res.*, **88**, 2565-2570, 1983.
- McGillicuddy, D. J., and A. R. Robinson, Eddy-induced nutrient supply and new production in the Sargasso Sea, *Deep Sea Res.*, **44**, 1427-1450, 1997.
- McGillicuddy, D. J., A. R. Robinson, D. A. Siegel, H. W. Jannasch, R. Johnson, T. D. Dickey, J. McNeil, A. F. Michaels, and A. H. Knap, Influence of mesoscale eddies on new production in the Sargasso Sea, *Nature*, **394**, 263-266, 1998.
- McGowan, J. A., and T. L., Hayward, Mixing and oceanic productivity, *Deep Sea Res.*, **25**, 771-793, 1978.
- Naderi, F. M., M. H. Freilich, and D. G. Long, Spaceborne radar measurement of wind velocity over the ocean: An overview of the NSCAT scatterometer system, *Proc. IEEE*, **79**, 850-866, 1991.
- Nelson, N. B., D. A. Siegel, and A. F. Michaels, Seasonal dynamics of colored dissolved organic material in the Sargasso Sea, *Deep Sea Res.*, **45**, 931-957, 1998.
- Odum, W. E., E. P. Odum, and H. T. Odum, Nature's pulsing paradigm, *Estuaries*, **18**, 547-555, 1995.
- Ondrusek, M. E., R. R. Bidigare, S. T. Sweet, D. A. Defreitas, and J. M. Brooks, Distributions of phytoplankton pigments in the North Pacific, *Deep Sea Res.*, **29**, 1451-1469, 1991.
- Oschlies, A., and V. Garçon, Eddy-induced enhancement of primary production in a model of the North Atlantic Ocean, *Nature*, **394**, 266-269, 1998.
- Platt, T., and W.G. Harrison, Biogenic fluxes of carbon and oxygen in the ocean, *Nature*, **318**, 55-58, 1985.
- Platt, T., S. Sathyendranath, O. Ulloa, W. G. Harrison, N. Hoepffner, and J. Goes, Nutrient control of phytoplankton photosynthesis in the western North Atlantic, *Nature*, **356**, 229-231, 1992.
- Scharek, R., M. Latasa, D. Karl, and R. R. Bidigare, Temporal variations in diatom abundance and downward vertical flux in the oligotrophic North Pacific gyre, *Deep Sea Res.*, **46**, 1051-1075, 1999.
- Siegel, D. A., A. F. Michaels, J. C. Sorensen, M. C. O'Brien, and M. A. Hammer, Seasonal variability of light availability and utilization in the Sargasso Sea, *J. Geophys. Res.*, **100**, 8695-8713, 1995.
- Smith, R. C., and K. S. Baker, Optical properties of the clearest natural waters (200-800 nm), *Appl. Opt.*, **20**, 177-184, 1981.
- Smith, R. C., K. J. Waters, and K. S. Baker, Optical variability and pigment biomass in the Sargasso Sea as determined using deep-sea optical mooring data, *J. Geophys. Res.*, **96**, 8665-8686, 1991.
- Steele, J. (Ed.), Some comments on planktonic patches, in *Spatial Patterns in Plankton Communities*, pp. 11-20, Plenum, New York, 1978.
- Strickland, J. D. H., and T. R. Parsons, *A Practical Handbook of Seawater Analysis*, 167 pp., Fish. Res. Board of Can., Ottawa, Ont., 1972.
- Strub, P. T., and C. James, Altimeter derived variability of surface velocities in the California Current system; 2, Seasonal circulation and eddy statistics, *Deep Sea Res.*, **47**, 831-870, 2000.
- Toplis, B. J., and T. Platt, Passive fluorescence and photosynthesis in the ocean: Implications for remote sensing, *Deep-Sea Res.*, **33**, 849-864, 1986.
- Walker, D. A., and C. B. Osmond, Measurement of photosynthesis in

- vivo using a leaf disk electrode: Correlations between light dependence steady-state photosynthetic  $O_2$  evolution and chlorophyll a fluorescence transients, *Proc. R. Soc. London B*, 227, 267-280, 1986.
- Weigert, R. G., and E. Penas-Lado, Nitrogen-pulsed systems on the coast of northwest Spain, *Estuaries*, 18, 622-635, 1995.
- Wentz, F. J., and D. K. Smith, A model function for the ocean-normalized radar cross-section at 14 GHz derived from NSCAT observations, *J. Geophys. Res.*, 104, 11,499-11,514, 1999.
- Wiggert, J., T. Dickey, and T. Granata, The effect of temporal undersampling on primary production estimates, *J. Geophys. Res.*, 99, 3361-3371, 1994.
- Winn, C. D., L. Campbell, J. R. Christian, R. M. Letelier, D. V. Hebel, J. E. Dore, L. Fujieki, and D. M. Karl, Seasonal variability in the phytoplankton community of the North Pacific Subtropical Gyre, *Global Biogeochem. Cycles*, 9, 605-620, 1995.
- Woods, J.D., Mesoscale upwelling and primary production, in *Toward a Theory of Biological-Physical Interactions in the World Ocean*, edited by B. J. Rothschild, pp. 7-38, Kluwer Acad., Norwell, Mass, 1988.
- M. R. Abbott, M. Freilich, R. M. Letelier, and T. Strub, College of Oceanic and Atmospheric Sciences, Oregon State University, 104 Ocean Admin. Bldg., Corvallis, OR 97331-5503 (mabbott@oce.orst.edu; mhi@oce.orst.edu; letelier@oce.orst.edu; pts@oce.orst.edu)
- P. Flament, D. M. Karl, and R. Lukas, School of Ocean and Earth Science and Technology, University of Hawaii, 1000 Pope Rd. MSB 208, Honolulu, HI 96822 (e-mail: dkarl@soest.hawaii.edu; pflament@soest.hawaii.edu; rlukas@soest.hawaii.edu)

(Received March 17, 1999; revised March 27, 2000; accepted August 22, 2000)